WPPMI-CPR(18) 20024

F Maviglia et al.

Electromagnetic modelling and design of DEMO and disruption location prediction

Preprint of Paper to be submitted for publication in Proceeding of
30th Symposium on Fusion Technology (SOFT)

This work has been carried out within the framework of the EUROfusion Consortium and has received funding from the Euratom research and training programme 2014-2018 under grant agreement No 633053. The views and opinions expressed herein do not necessarily reflect those of the European Commission.

Optimization of DEMO geometry and disruption location prediction

Francesco Maviglia[a,b], Raffaele Albanese[b], Roberto Ambrosino[b], Christian Bachmann[a], Gianfranco Federici[a].

[a]*EUROFusion PMU, Boltzmannstr. 2, Garching 85748, Germany*
[b]*Consorzio CREATE, Univ. Napoli Federico II - DIETI, 80125 Napoli, Italy*

The design study of DEMO is one of the main points of the European Roadmap to Fusion Electricity. The present pre-conceptual design phase of DEMO is used to explore a flexible range of the main machine geometrical design parameters and plasma scenarios. This paper presents the electromagnetic (EM) modelling of the DEMO baseline scenario, including the optimization activities on the plasma surrounding electrically conductive structures and their influence on the passive vertical stabilization (VS). The design of the first wall (FW) poloidal geometry was performed taking into account the charged particle heat loads in order to minimize the distance between the plasma and the electrically conductive structures. The improvements on the passive and active VS allowed increasing the maximum controllable plasma elongation, with a consequent increase on the fusion performance. Finally, a study is presented on the possibility to predict the plasma final position following a vertical displacement event (VDE). This prediction capability supports the development of a wall protection strategy from plasma transients. A model is presented based on the assumptions on the characteristic time constants expected for the current quench (CQ) time and *L/R* time constant of the conductive structures.

Keywords: DEMO, electromagnetic modelling, vertical stabilization, disruption simulations.

1. Introduction

The design study of a DEMOnstration (DEMO) Fusion Plant is one of the main points of the European Roadmap to Fusion Electricity [1]. The pre-conceptual design phase of DEMO is presently used to explore a range of the main machine design parameters, using as a preliminary step system codes [2, 3, 4], which capture the main dependencies of the physics and engineering parameters with the machine geometry. The resulting DEMO baseline design is then used to perform analyses with specific engineering and physics codes. This paper presents the EM modelling of the DEMO baseline scenario, including the analysis and design activities on the plasma surrounding electrically conductive structures, and their influence on the VS, which is one of the most critical aspects to be considered in elongated plasmas. A careful design of the blanket FW poloidal geometry was derived, based on [5], considering the plasma charged particle heat load on the wall. This allowed minimizing the distance between the plasma and the vacuum vessel (VV), which is the closest electrically conductive and toroidally continuous structure. The improvements of both the passive and active [6] VS allowed to increase the maximum controllable plasma elongation at 95% of the separatrix, named κ_{95}, resulting in an increase on fusion power. A study was also performed on the possibility to predict the plasma final position after a VDE. This is important as in the protection strategy of the DEMO FW areas need to be identified where the plasma may come in contact with the plasma intransient events. The ITER whole wall limiter approach is not applicable to DEMO [5].

2. DEMO 2D poloidal geometry optimization

During the present pre-conceptual design phase of the DEMO project, system codes [2, 3, 4] are used to capture the effect of the main plasma and machine parameters on the overall radial and vertical build. The approach to define a single reference configuration, described in [7], is applied to ensure consistency of all DEMO studies with this initial design point. In recent studies [8] the large effect of the variation of *+/-10%* of the κ_{95} was shown, leading to a corresponding variation on the system code solution on the fusion power performances, and hence on the overall net electric power, $P_{el,net}$, respectively of *+125% / -75%*. In contrast, more elongated plasmas have a detrimental effect on the VS control, as they have a higher vertical velocity growth rate γ. An optimization was performed with the aim of reducing the distance between the plasma and the closest electrically conductive structures, which has a beneficial effect on the passive VS, while taking into account the heat flux to the plasma facing components due to charged particles and the radiation loads. An optimized 2D poloidal geometry of the FW shape was obtained, using the methodology developed in [5], such as to satisfy the total predicted heat flux below $1MW/m^2$, representing the approximate FW steady state technological limit [9].The thickness of the breeding blanket (BB) on the outboard was reduced from *1.3m* to *1.0m*, effectively reducing the distance between plasma and VV [10]. A number of EM models were evaluated including the optimized poloidal shape of the VV to assess the effect on the vertical velocity growth rate γ. The different models had a κ_{95} in the range from *1.59*, as the previous non optimized baseline, up to *1.7*.

3. DEMO Vertical stability performances

The criteria used to evaluate the maximum controllable elongation were chosen as follow:

1) *Passive stabilization*: The stability margin m_s, defined as in [11, 12], has to be $\geq$ *0.3*.
2) *Active stabilization*: The power required to stabilize a 5cm vertical VDE has to be $\leq$ *500MW*, using the

author's email: francesco.maviglia@euro-fusion.org

best achievable performance controller, *i.e.* by applying a voltage in the control circuit, immediately after the perturbation, equal to 5 to 10 times the voltage V_0 required to stabilize the plasma for $t \to \infty$.

The active ex-vessel coils control power limit of *500MW* was chosen scaling up the corresponding ITER value of *200MW* of power required by the VS system using ex-vessel coils [13]. A further conservative margin was also added because ITER uses a realistic controller and measurement noise estimations, which have not been introduced for DEMO simulation yet, and will have a detrimental effect. The most challenging configuration for the VS control in a DEMO pulse is the start of ramp down (SRD), characterized by high internal inductance (li=1), low poloidal beta (β_{pol}=0.1), and consequently the lowest stability margin and highest control power required. For this reason it was chosen to evaluate the maximum controllable elongation. The results, reported in Tab. 1, show that the VS performances obtained with the optimized DEMO configuration with κ_{95}=*1.65*, satisfy the requirement set in the criterion 1), in terms of passive stabilization parameters m_s. Also the active stabilization criterion 2) is fulfilled for what concerns the total power required by the VS system P_{VS}, for a 5cm VDE. The maximum vertical displacement, Z_{max}, was up to *6.8cm* using the best achievable performance controller with $5V_0$-$10V_0$, which allows avoiding the plasma – FW contact.

γ [s^{-1}]	m_s	Z_{max} [cm]	P_{VS} [MW]
6.7	0.48	6.8 - 6.1	210 -540

Tab. 1 VS performances for the optimized DEMO geometry with κ_{95}=*1.65*, for the SRD configuration using the best achievable performance controller with $5V_0$-$10V_0$.

An additional optimization activity was performed in parallel on the active VS. This is represented by the optimization of the plasma equilibria, via minimization of the distance between plasma current centroid and magnetic axis, which decreases the plasma perturbation coupling with the vertical plasma movement, and is reported in detail in [6]. As a consequence of these studies it was possible to increase the maximum controllable κ_{95} from *1.59* to *1.65*. An example of the resulting magnetic equilibrium optimization is shown in Fig. 1.

4. Prediction of plasma final position after a vertical displacement event (VDE)

The protection strategy of DEMO FW from plasma transient was chosen to be one of eight "key design issues" (KDI), identified as critical, because the ITER solution, i.e. a FW designed for plasma-wall contact, is not feasible in DEMO [14]. The DEMO FW is a thin structure in order to minimize the reduction of neutron flux onto the tritium breeding zone inside the BB. The present design foresees a 2mm thin tungsten armor covering an array of small-scale parallel cooling channels made of EUROfer [9]. This BB FW can withstand steady state heat fluxes up to about 1MW/m^2 [9]. Due to its thin-walled structure it offers however only a small thermal buffer against high short-term heat fluxes that typically occur in case of plasma-wall contact during plasma transients.

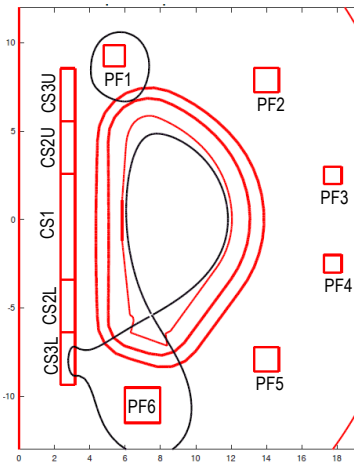

Plasma param.	SOF
I_{pl} [MA]	19.1
L_i	1.14
β_{pol}	0.8
R_{pl} [m]	9.19
Z_{pl} [m]	0.08
R_{axis} [m]	9.39
Z_{axis} [m]	0.03
a [m]	2.88
B_{tor} @axis [T]	4.89
$beta_n$	0.03
q_{95}	2.93
k_{95}	1.65
δ_{95}	0.33
Perimeter [m]	25
Volume [m^3]	2355
γ [s^{-1}]	2.4

Fig. 1 DEMO optimized geometry and main parameters for the Start Of Flat top (SOF) phase, based on 2017 baseline.

During the most severe disruptive events, it is calculated that an energy level of the order of *1.3GJ* [15] could be released during the thermal quench (TQ) to the wall within few *ms*. Even impact heat loads 1-2 order of magnitude lower in energy exceed the tolerable limit of the BB FW [5]. A strategy based on the use of discrete high heat flux limiters is hence being proposed and developed for DEMO. It is therefore required to be able to predict locations of plasma-wall contact during disruptions in DEMO to guide the definition of the configuration of limiters capable to protect the BB FW. An EM analysis using dynamic models of active and passive conductive structures is able to predict all the possible points of the FW where the plasma could end up after a fast transient. This approach has already been proposed and successfully tested during breakdown, another phase when the plasma current is low [16, 17]. The main assumption regards the ratio between the plasma CQ time (τ_D) and the *L/R* time constants of the conductive structures, i.e. the VV and control coil circuits, with the respective time constants τ_V, *and* τ_C. Two different cases are analyzed in the following paragraphs.

4.1 Model for $\tau_D \ll \tau_V$

For this case the main assumption is that the disruption CQ time is much faster than the *L/R* time constant of the vessel, *i.e.* $\tau_D \ll \tau_V$. Under these conditions the VV behaves as a perfect conductor keeping the poloidal flux frozen. The magnetic flux at the end of the disruption can be obtained by solving the magnetostatic problem in the vacuum inside the vessel, with Dirichlet boundary conditions on the poloidal flux before the disruption, *i.e.* with the plasma in nominal conditions. The location where the plasma ends up is characterized by a force perpendicular to the wall and pushing the plasma against it. If this is not verified a tangential component of the force would make the plasma slide towards another location. Thus, the vacuum magnetic field should be tangential to the wall with a counterclockwise orientation. A final condition is the

stability of the location, related to the local curvature of the field and of the FW: The tangential force in the neighborhood should be such as to make the plasma slide toward the location. These conditions are verified by the local maxima of the poloidal magnetic flux on the FW.

4.2 Model for τ_D comparable with τ_V

The time scales of interest for the DEMO case are:

- The CQ time of the plasma disruption, τ_{CQ}: this is assumed to range between the fastest at *74ms*, as reported in [18] to the slowest, considering the recent results with metallic wall in JET and ASDEX-U [19, 20, 21], scaled for DEMO plasmas, up to *200ms*.
- The *L/R* time constant of the vessel τ_V, which is obtained as the longest time constant of the system without plasma: in DEMO *478ms* with all the Central Solenoid (CS) and Poloidal Field (PF) coils in short circuit (the most realistic case, see below), or *858ms* if keeping all PF coil current constant;
- The characteristic time of the PF coil system τ_C: we estimate this figure as the time needed by the power supplies to get the same current variation produced in the coils (supposed in short circuit) at the end of the transient following a disruption:

  $$\tau_{Ck} = (L\,\Delta I)_k / V_k = M_{kp}\, I_p / V_k$$

  where L is the inductance matrix, I_k is the k_{th} coil current, V_k is the voltage limit for the k_{th} coil, M_{kp} is the mutual inductance between the k_{th} coil and the plasma, and I_p is the plasma current.

In DEMO the fastest time constant is longer than *1.3s*, *i.e.* by a factor of 6 larger than the quench time, see Tab. 2. The CS/PF coils therefore behave as perfect conductors keeping the poloidal flux frozen.

	R[m]	Z[m]	ΔR[m]	ΔZ[m]	N_{turns}	V_{max}[kV]	M_p[mH]	M_pI_p [kVs]	M_pI_p/V_{max} [s]
CS3U	2.77	7.07	0.8	2.99	860	6	0.70	13.3	2.22
CS2U	2.77	4.08	0.8	2.99	860	6	1.11	21.2	3.53
CS1	2.77	-0.4	0.8	5.97	1720	12	2.88	54.9	4.58
CS2L	2.77	-4.88	0.8	2.99	860	6	0.99	18.9	3.15
CS3L	2.77	-7.86	0.8	2.99	860	6	0.61	11.7	1.94
PF1	5.4	9.26	1.15	1.15	370	10	0.71	13.6	1.36
PF2	14	7.9	0.85	0.85	202	10	1.41	26.9	2.69
PF3	17.87	2.5	1.1	1.1	309	10	2.87	54.9	5.49
PF4	17.87	-2.5	1.1	1.1	309	10	2.87	54.9	5.49
PF5	14	-7.9	1.2	1.2	403	10	2.81	53.8	5.38

Tab. 2 CS/PF coil system, mutual inductance with the plasma (a filament of *19.1MA* located at *R=8.9 m*, *Z=0*), and estimation of characteristic time of the circuits $\tau_{Ck} = M_{kp}\, I_p / V_k$

Contrary to the PF coil system, the time constant of the VV is not much longer than the CQ time. This means that the flux is not conserved perfectly in the vessel. To estimate the fraction of the flux not shielded by the vessel we consider the simple first order system:

$$L_v\, dI_v/dt + R_v\, I_v = - M_{vp}\, dI_p/dt \qquad (1)$$

where L_v is the vessel inductance, I_v is the vessel current, t is the time, R_v is the vessel resistance, M_{vp} is the mutual inductance between plasma and vessel ($M_{vp} = L_v$ assuming perfect coupling).

For a linear plasma current decay in the CQ time τ_D, in the time interval $(0, \tau_D)$ we can write:

$$dI_v/dt + I_v/\tau_v = I_p/\tau_D \quad in\ (0,\ \tau_D) \qquad (2)$$

and at the final time instant we get:

$$I_v(\tau_D) = (\tau_v\, I_p/\tau_D) \cdot [1 - exp(-\tau_D/\tau_V)] \qquad (3)$$

4.3 Sensitivity of disruption locations to the quench time τ_D for DEMO configurations

Extrapolating to DEMO the possible characteristic CQ time, it is possible to apply the models presented in sections 4.1 and 4.2 to estimate the final location of the plasma after a disruption. By applying the equation (3), the figures for DEMO indicate that the vessel current at the end of the quench is:

- 100% of Ip for $\tau_D \to 0$;
- 91% of Ip for $\tau_D = 74\ ms$;
- 79% of Ip for $\tau_D = 200\ ms$;
- 0% of Ip for $\tau_D \to \infty$.

To find the plasma final location in the case $\tau_D \to 0$ ($\tau_D << \tau_v$) the procedure described in Section 4.1 is applied, freezing the flux linked to the vessel. In the case $\tau_D \to \infty$ ($\tau_D >> \tau_v$) we apply the same procedure, but this time freezing only the flux linked to the external coils. In other cases, the flux maps are approximated via linear interpolation between the two limit cases. The two extreme cases for $\tau_D << \tau_V$ and $\tau_D >> \tau_V$ are shown in Fig. 2; the possible final locations of the plasma are shown in black asterisks. Other locations where the vacuum field is tangential are discarded, either because the force would push the plasma away from the wall or because they would be unstable, as the force in the neighborhood would make the plasma slide away from the location. The upper possible locations are very similar, due to the curvature of the FW in the upper zone moves, and they move from *R=6.7m*, *Z=5.7m*, in the first case, to *R=6.5m*, *Z =5.5m* in the second case.

It has to be noted that with this procedure is possible to anticipate the possible final locations of the plasma at the end of the CQ. This is important to design the FW and the wall protection limiters in these areas when, during the CQ: (i) part of the plasma magnetic energy is being partially converted in thermal energy [21], or (ii) is used to accelerate the electrons to relativistic speed, producing runaway electrons (REs) beams impacting the wall. The latter is presently regarded as one of ITER's and DEMO's open issues also because techniques developed in present experiments to actively control the beams with ex-vessel coils [22, 23] may not be available in ITER and DEMO due to the higher field penetration time through the vessel. To evaluate the locations where the plasma first touches the plasma-facing components during a disruptive event, where the TQ occurs, a transient simulation is needed, as presented in [6].

4.4 Results and future work

The results presented in the previous sections show that the final plasma location after a disruption CQ depends on the plasma equilibrium shape, the geometry of the plasma facing components (PFCs) and the characteristic times of the problem. These results were also verified with nonlinear dynamic simulations, as presented in [6], using the 2D CREATE NL code [24]. At present, in the cases analyzed for DEMO, the location

is nearly the same for: 1) SOF and EOF plasmas, 2) plasma with very different CQ times, and 3) plasma with triangularity values ranging from 0.37 to 0.45, as from [5, p. 388]. To avoid the final contact point between plasma and wall to be located in regions that can hardly be protected by a replaceable limiter integrated in a VV port, the equilibrium configuration and the geometry of the PFCs should properly be designed, so as to have the final vacuum field parallel to the PFCs in the desired region. The possibility to add these requirements into the DEMO equilibria and geometry design will be explored in the future work.

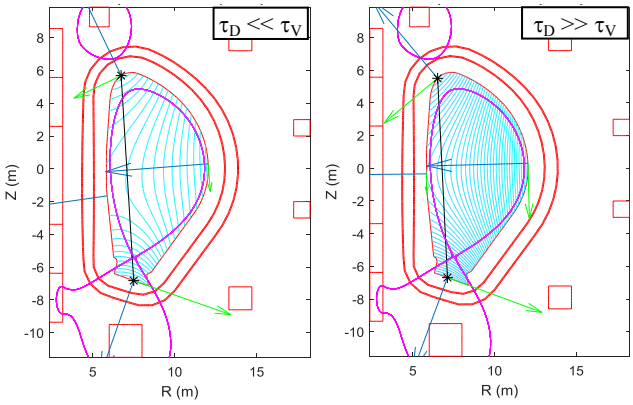

Fig. 2 DEMO at SOF: Possible locations of plasma final position (black asterisks) on the FW (local magnetic field in green, local force in cyan) for the two extreme quench times $\tau_D << \tau_V$, on the left, and $\tau_D >> \tau_V$, on the right.

5 Conclusions

In this paper the optimization of some of the DEMO machine's geometrical parameters is presented. The methodologies developed in recent years have been applied to minimize the distance between the plasma and the passive conductive structures, such as BB and VV, by shaping the FW in order to obtain a heat flux level during nominal conditions compatible with the present technology limits. This optimization allowed enhancing the DEMO passive VS performances, which, together with the plasma scenario optimization [6] allowed increasing the maximum controllable plasma elongation κ_{95} from *1.59* to *1.65*, with a large positive impact on the fusion power. This was obtained while fulfilling the constraints on the stability margin, $m_s \geq 0.3$ in all the foreseeable plasma conditions, and the limitation on the maximum active power $\leq$ *500MW* needed to recover a 5cm VDE, preliminary scaled from ITER. The resulting new DEMO baseline is characterized by a reduced machine radial build, one of the main indicators of the overall cost. Finally a methodology was proposed on the possibility to predict the final location of the plasma after a disruption CQ following a VDE, by evaluating the plasma magnetic flux map in nominal conditions, *i.e.* before the disruption. Two simple EM models were proposed applicable to the *L/R* time constant of the conductive structures much larger or much smaller than the time constant of the disruption. In DEMO the two time constants do not differ strongly (the disruption CQ time is predicted in the range *74ms* [18] to *200ms* [19, 20], the L/R time of the conductive structures is in the range *400ms* to *800ms*). Hence for many cases both models are applied via a linear combination according to equation (3). For the analyzed cases the final location did not change much between start and end of flattop, with different triangularity or with opposite extreme time constants, *i.e.* $\tau_D << \tau_V$ or $\tau_D >> \tau_V$, and are in line with the transient simulation carried out for DEMO. This approach could be used in the future to attempt to use the available degrees of freedom to design the plasma and machine geometry to ensure that the final vacuum field would be parallel to the PFCs in the region where is possible to foresee the installation of a replaceable protecting limiter. This would avoid damage to the standard PFCs during the CQ by the heat flux due to the plasma magnetic energy being partially transformed in thermal energy and deposited via charged particle, or by REs beam.

Acknowledgments

This work has been carried out within the framework of the EUROfusion Consortium and has received funding from the Euratom research and training programme 2014-2018 under grant agreement No 633053. The views and opinions expressed herein do not necessarily reflect those of the European Commission.

References

[1] F. Romanelli, et al., "Fusion Electricity A roadmap to the realisation of fusion energy".
[2] M. Kovari, et al., *FED*, vol. 89, no. 12, 2014.
[3] M. Kovari, et al., *FED*, vol. 104, p. 9–20, 2016.
[4] C. Reux, et al., *NF*, vol. 55, p. 073011, 2015.
[5] F. Maviglia, et al., *FED*, vol. 124, p. 385, 2017.
[6] R. Ambrosino, et al., *This conference.*
[7] G. Federici, et al., *FED*, 2018 (in press).
[8] R. Wenninger, et al., *NF*, vol. 57, p. 016011, 2017.
[9] F. Cismondi, et al, *FED*, 2018 (in press).
[10] C. Bachmann, et. al, *FED*, no. In Press, 2018.
[11] F. Hofmann, et al., *NF*, vol. 42, p. 743, 2002.
[12] Q Jin-Ping, et al., *Chin. Phys. B*, p. 2432, 2009.
[13] Y. Gribov, et al., *NF*, vol. 55, p. 073021, 2015.
[14] C. Bachmann, et al., *This conference.*
[15] R. Wenninger, et al., *NF*, vol. 57, p. 046002, 2017.
[16] F. Maviglia et al., *FED*, vol. 86, no. 6–8, p. 675, 2011.
[17] F. Maviglia et al., *IEEE Trans. Mag*, vol. 50(2), 2014.
[18] C. Bachmann, et al., *FED*, vol. 124, pp. 633-637, 2017.
[19] P. C. de Vries, et al., *PPCF*, vol. 54, 2012.
[20] R. Neu, et al., *IEEE Trans. Plas. Sci.*, vol. 42, 2013.
[21] M. Lehnen, et al., *NF*, Vols. 53, N. 9, p. 93007, 2013.
[22] N. W. Eidietis, et al., *Phys. plas.*, vol. 19, p. 56109, 2012.
[23] B. Esposito, et al., *PPCF*, vol. 59, p. 014044, 2017.
[24] R.Albanese, et al., *FED*, vol. 96–97, p. 664, 2015.